

QubitE: Qubit Embedding for Knowledge Graph Completion

Anonymous ACL submission

Abstract

Knowledge graph embeddings (KGEs) learn low-dimensional representations of entities and relations to predict missing facts based on existing ones. Quantum-based KGEs utilise variational quantum circuits for link prediction and score triples via the probability distribution of measuring the qubit states. However, there exists another best measurement for training variational quantum circuits. Besides, current quantum-based methods ignore theoretical analysis which are essential for understanding the model performance and applying for downstream tasks such as reasoning, path query answering, complex query answering, etc. To address measurement issue and bridge theory gap, we propose QubitE whose score of a triple is defined as the similarity between qubit states. Here, our measurements are viewed as kernel methods to separate the qubit states, while preserving quantum advantages. Furthermore, we show that (1) QubitE is full-expressive; (2) QubitE can infer various relation patterns including symmetry/antisymmetry, inversion, and commutative/non-commutative composition; (3) QubitE subsumes several existing approaches, *e.g.* DistMult, pRotatE, RotatE, TransE and ComplEx; (4) QubitE owns linear space complexity and linear time complexity. Experiments results on multiple benchmark knowledge graphs demonstrate that QubitE can achieve comparable results to the state-of-the-art classical models.

1 Introduction

Knowledge graphs (KGs) consist of nodes (entities) and edges (relationships between entities), which have been widely applied for knowledge-driven tasks such as question answering, recommendation system, and search engine. However, KGs are incomplete and this problem affects the performance of any algorithm related to KGs. Knowledge graph embeddings (KGEs) are prominent approaches to predict missing links for KG completion.

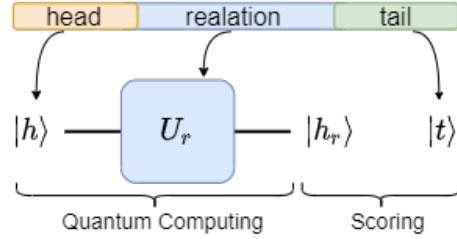


Figure 1: Visualization of the QubitE architecture.

Quantum-based KGE is the application of quantum mechanics on knowledge graph completion (KGC) field, but current research is still in its initial stage. The most classical quantum-based KGE is proposed by Ma et al. (2019) using parametric quantum circuits. Specially, Ma et al. (2019) proposes two types of variational quantum circuits KGEs. The first type, *i.e.* QCE, considers latent features for entities as coefficients of quantum states, while predicates are characterized by parametric gates acting on the quantum states. The score of a triple depends on measurements on quantum states. The quantum advantages, *e.g.* normalization constraint of quantum states and quantum gates, disappear when optimizing the model. The second type, *i.e.* F-QCE, generates embeddings of entities from parameterized quantum gates acting on the pure quantum states. The quantum embeddings can be trained efficiently meanwhile preserving the quantum advantages.

These two types perform a hybrid quantum-classical optimization procedure to optimize the parameters of quantum gates. However, recent studies (Schuld, 2021; Heredige et al., 2021) show that this strategy can be fundamentally formulated as a quantization of classical kernel methods, *e.g.* support vector machines (SVM) (Schölkopf et al., 2002), which implicitly separates the data according to their classes in a high-dimensional Hilbert space. The quantum feature map is taken

to be a fixed circuit, and the training adapts the measurement basis. By contrast, we note that if the entities are well-separated in Hilbert space, the best measurements, that distinguish whether the entities are the tails of the tuple $(h, r, ?)$ or not, are known as follows: The best measurement for the entities separated by the trace distance is the Helstrom minimum error measurement, and the best measurement for the Hilbert-Schmidt distance is the fidelity or overlaps measurement between the semantics of embedded entities. Therefore, we argue that, the adaptive training of the quantum circuit should focus on the metric that carries out a maximally separating embedding.

In this paper, we propose a new quantum-based KGE for knowledge graph completion to explore the performance of different measurements. We numerically investigate different measurements for training quantum embeddings on four standard datasets. Extensive experiments demonstrate the efficacy of our model.

In addition, we analyze our model theoretically, including *subsumption*, *full expressiveness*, *patterns inference* and *space&time complexity*. We prove that QubitE is *fully expressive* and deriving a bound on the embedding dimensionality for full expressiveness, which is the crucial property that indicates well-separation of the data. We show that QubitE subsumes TransE, RotatE, pRotatE, ComplEx and DisMult. We also prove that QubitE allows to learn composition, inverse and symmetric relation patterns. Besides, QubitE owns linear space complexity and linear time complexity.

We summarise our contributions as follows:

- **KGE:** We propose QubitE, a new *linear* quantum-based KGE model for link prediction on knowledge graphs, that is simple and expressive to explore the performance of different measurements.
- **Theoretical Analysis:** We fully analyze QubitE theoretically in *subsumption*, *full expressiveness*, *patterns inference* and *space&time complexity*.
- **Experiments:** We conduct extensive experiments on four standard public datasets to demonstrate the efficacy of our model. The source code is available online ¹.

¹<https://github.com/LinXueyuanStudio/QubitE>

2 Related Work

The KG embedding is divided into the following categories, Euclidean geometric model, non-Euclidean geometric model, tensor decomposition model, neural network model, etc.

Euclidean KG Embedding.

TransE (Bordes et al., 2013) models the relationship as a distance transformation from the head entity to the tail entity; **TransR** (Lin et al., 2015) proposes to design a projection matrix for each relationship, in order that entities have different embedding vectors under different relationships; **RotatE** (Sun et al., 2019) defines the relationship as rotation transformation from head entities to tail entities in the two-dimensional complex space; **QuatE** (Zhang et al., 2019) uses the quaternion method to extend the rotation to three-dimensional complex space; **5*E** (Nayyeri et al., 2021) proposes a model based on projective geometry that provides a unified method for simultaneously representing translation, rotation, homomorphism, inversion, and reflection.

Non-Euclidean KG Embedding.

MuRP (Balazevic et al., 2019b) models both in hyperbolic space and Euclidean space, and combines relationship vectors, which can handle the multiple types of relationships that exist in the graph; **ATTH** (Chami et al., 2020) uses the expressiveness of hyperbolic space and attention-based geometric transformation to learn improved KG representation in low-dimensional space.

Tensor Decomposition KG Embedding.

DistMult (Yang et al., 2015) relaxes the constraint on the relationship matrix and uses a diagonal matrix to represent the relationship matrix; **Complex** (Trouillon et al., 2016) extends to the complex space, which can solve both symmetric and asymmetric relationships at the same time; **Simple** (Kazemi and Poole, 2018) proposed a simple Canonical Polyadic (CP) enhancement to allow the two embeddings of each entity to be learned independently; **HypER** (Balazevic et al., 2019a) uses a hypergraph network to generate a one-dimensional convolution filter for each relationship, in order to extract the specific characteristics of the relationship; **TuckerER** (Balazevic et al., 2019c) proposes a model that uses Tucker decomposition to perform link prediction on the binary tensor representation of KG.

Neural Network KG Embedding.

ConvE (Dettmers et al., 2018) uses a convolu-

tional neural network to define the scoring function; **CoPER** (Stoica et al., 2020) generates contextual parameters into neural network to predict links.

Quantum Embedding.

Ma et al. (2019) proposes two types of variational quantum circuits (**QCE** and **F-QCE**) for knowledge graph embedding. Lloyd et al. (2020) proposes a quantum embedding model that represents classical data points as quantum states in a Hilbert space via quantum feature map. A classical datapoint x is translated into a set of gate parameters in a quantum circuit ψ , creating a quantum state $|x\rangle$ such that $\psi : x \rightarrow |x\rangle$. However, our method is quite different. Firstly, we compare the quantum states via trace distance rather than the probability distribution of measuring the qubit states. Secondly, entities in KG are assigned tunable parameters directly to create quantum states instead of using parametric quantum circuits.

3 Preliminaries

Knowledge Graph Embeddings. A KG is a multi-relational directed graph $\mathcal{KG} = (\mathcal{E}, \mathcal{R}, \mathcal{T})$ where \mathcal{E} is the set of nodes (entities) and \mathcal{R} is the set of edges (relations between entities). The set $\mathcal{T} = \{(h, r, t)\} \subseteq \mathcal{E} \times \mathcal{R} \times \mathcal{E}$ contains all triples as (*head, relation, tail*), e.g. (*smartPhone, hypernym, iPhone*). To apply learning methods on KGs, a KGE learns vector representations of entities (\mathcal{E}) and relations (\mathcal{R}). A vector representation denoted by $(\mathbf{h}, \mathbf{r}, \mathbf{t})$ is learned by the model per triple (h, r, t) , where $\mathbf{h}, \mathbf{t} \in \mathbb{V}^{d_e}$, $\mathbf{r} \in \mathbb{V}^{d_r}$ (\mathbb{V}^d is a d -dimensional vector space). TransE (Bordes et al., 2013) considers $\mathbb{V} = \mathbb{R}$ while ComplEx (Trouillon et al., 2016) and RotatE use $\mathbb{V} = \mathbb{C}$ (complex space) and QuatE (Zhang et al., 2019) considers $\mathbb{V} = \mathbb{H}$ (quaternion space). In this paper, we choose two-dimensional Hilbert space to embed the graph i.e. $\mathbb{V} = \mathbb{C}^2$. Most KGE models are defined via a relation-specific transformation function $g_r : \mathbb{V}^{d_e} \rightarrow \mathbb{V}^{d_e}$ which maps head entities to tail entities, i.e. $g_r(\mathbf{h}) = \mathbf{t}$. On top of such a transformation function, the score function $f : \mathbb{V}^{d_e} \times \mathbb{V}^{d_r} \times \mathbb{V}^{d_e} \rightarrow \mathbb{R}$ is defined to measure the plausibility for triples: $f(\mathbf{h}, \mathbf{r}, \mathbf{t}) = p(g_r(\mathbf{h}), \mathbf{t})$. Generally, the formulation of any score function can be either $p(g_r(\mathbf{h}), \mathbf{t}) = -\|g_r(\mathbf{h}) - \mathbf{t}\|$ or $p(g_r(\mathbf{h}), \mathbf{t}) = \langle g_r(\mathbf{h}), \mathbf{t} \rangle$.

Qubit. A classical bit can exist in one of two states denoted as 0 and 1. A quantum bit or qubit can exist not only in these two discrete states but in all

possible linear superpositions of them. Mathematically, the quantum state of a qubit is represented as a state vector in a two-dimensional Hilbert space \mathbb{C}^2 , whose basis vectors are denoted in the Dirac notation as

$$|0\rangle = \begin{pmatrix} 1 \\ 0 \end{pmatrix}, |1\rangle = \begin{pmatrix} 0 \\ 1 \end{pmatrix} \quad (1)$$

Let the vector $|0\rangle$ correspond to the classical value 0, while $|1\rangle$ to 1. The state vector of a qubit is written as

$$|\psi\rangle = \mathbf{a}|0\rangle + \mathbf{b}|1\rangle \quad (2)$$

where $\mathbf{a}, \mathbf{b} \in \mathbb{C}$, $|\mathbf{a}|^2 + |\mathbf{b}|^2 = 1$. The complex numbers \mathbf{a} and \mathbf{b} are called quantum amplitudes. According to quantum mechanics, if we make measurement on $|\psi\rangle$ to see whether it is in $|0\rangle$ or $|1\rangle$, the outcome will be 0(1) with the probability $|\mathbf{a}|^2(|\mathbf{b}|^2)$ and state $|0\rangle(|1\rangle)$ immediately. The density matrix ρ of state $|\psi\rangle$ is given by:

$$\rho = |\psi\rangle \langle \psi| \quad (3)$$

Quantum Gates. Quantum gates essentially transform the system from one state to another state. When measurements are not made, the time evolution of a state is described by the Schrödinger equation. Because of the probabilistic interpretation of quantum mechanics, state vectors are normalized to 1. Thus the time development is unitary. Quantum gate U holds $UU^\dagger = U^\dagger U = I$, where U^\dagger is the conjugate transpose of matrix U . The general expression of a 2×2 unitary matrix is

$$U = \begin{pmatrix} \mathbf{a} & -e^{i\psi}\mathbf{b}^* \\ \mathbf{b} & e^{i\psi}\mathbf{a}^* \end{pmatrix} \quad (4)$$

where $\mathbf{a}, \mathbf{b} \in \mathbb{C}$, $|\mathbf{a}|^2 + |\mathbf{b}|^2 = 1$ and ψ is the angle. \mathbf{a}^* is the complex conjugate of \mathbf{a} .

4 Method

4.1 Model Formulation

Given a triple (h, r, t) , the head and tail entities $h, t \in \mathcal{E}$ are embedded into a d dimensional Hilbert space i.e. $\mathbf{h}, \mathbf{t} \in \mathbb{C}^{2d}$ where each element is a 2-dimensional complex value vector. A relation $r \in \mathcal{R}$ is embedded into a d dimensional vector \mathbf{r} where each element is a 2×2 complex value unitary matrix. \mathbf{r} contains two complex vectors \mathbf{r}_a and $\mathbf{r}_b \in \mathbb{C}^d$. With $\mathbf{r}_{ai}, \mathbf{r}_{bi}, \mathbf{h}_{ai}, \mathbf{h}_{bi}, \mathbf{t}_{ai}, \mathbf{t}_{bi}$, we refer to the i th element of $\mathbf{r}_a, \mathbf{r}_b, \mathbf{h}_a, \mathbf{h}_b, \mathbf{t}_a, \mathbf{t}_b$ respectively.

4.1.1 Entity-specific Qubit Embedding

We use standard representation of the state of qubit to represent an entity in \mathbb{C}^{2d} . The i th element of entity embedding vector \mathbf{h} is given by

$$\mathbf{h}_i = \mathbf{h}_{ai} |0\rangle + \mathbf{h}_{bi} |1\rangle = \begin{pmatrix} \mathbf{h}_{ai} \\ \mathbf{h}_{bi} \end{pmatrix}, \quad (5)$$

$$i = 1, 2, \dots, d$$

where d is entity embedding dimension, $\mathbf{h}_{ai}, \mathbf{h}_{bi} \in \mathbb{C}$ and $|\mathbf{h}_{ai}|^2 + |\mathbf{h}_{bi}|^2 = 1$ such that $\mathbf{h} = [\mathbf{h}_1, \mathbf{h}_2, \dots, \mathbf{h}_d]$.

Respectively, the density matrix of entity h is

$$\rho_{\mathbf{h}_i} = |\mathbf{h}_i\rangle \langle \mathbf{h}_i|$$

$$= \begin{pmatrix} |\mathbf{h}_{ai}|^2 & \mathbf{h}_{ai} \mathbf{h}_{bi}^* \\ \mathbf{h}_{bi} \mathbf{h}_{ai}^* & |\mathbf{h}_{bi}|^2 \end{pmatrix}. \quad (6)$$

4.1.2 Relation-specific Quantum Gate

We use relation-specific transformation to map the head entity \mathbf{h} from a source to a target Hilbert space. Since quantum gates are unitary, we write the parameterized unitary matrix of i th element of relation embedding vector \mathbf{r} as

$$\mathbf{r}_i = \mathcal{U}_{ri} = \begin{pmatrix} \mathbf{r}_{ai} & -e^{i\psi} \mathbf{r}_{bi}^* \\ \mathbf{r}_{bi} & e^{i\psi} \mathbf{r}_{ai}^* \end{pmatrix}, \quad (7)$$

$$i = 1, 2, \dots, d$$

where d is relation embedding dimension, $\mathbf{r}_{ai}, \mathbf{r}_{bi} \in \mathbb{C}$ and $|\mathbf{r}_{ai}|^2 + |\mathbf{r}_{bi}|^2 = 1$ so that $\mathbf{r} = [\mathbf{r}_1, \mathbf{r}_2, \dots, \mathbf{r}_d]$. This implies $\det(\mathcal{U}_{ri}) = e^{i\psi} \neq 0$ *i.e.* \mathcal{U}_{ri} is invertible.

To apply quantum gate to the qubit, *i.e.* to apply relation-specific transformation \mathbf{r} to the head entity \mathbf{h} , we perform element-wise transformation via matrix multiplication to compute the transformed entity representation \mathbf{h}_r :

$$\mathbf{h}_{ri} = g_{ri}(\mathbf{h}_i) = \mathcal{U}_{ri} \mathbf{h}_i = \begin{pmatrix} \mathbf{r}_{ai} \mathbf{h}_{ai} - e^{i\psi} \mathbf{r}_{bi}^* \mathbf{h}_{bi} \\ \mathbf{r}_{bi} \mathbf{h}_{ai} + e^{i\psi} \mathbf{r}_{ai}^* \mathbf{h}_{bi} \end{pmatrix},$$

$$i = 1, 2, \dots, d \quad (8)$$

which implies $\mathbf{h}_r = [\mathbf{h}_{r1}, \mathbf{h}_{r2}, \dots, \mathbf{h}_{rd}]$.

4.1.3 Score Function

In our method, we do not need to exactly measure the states. Instead, we separate the states by kernel methods.

The score of a triple in KG is the similarity $\langle \mathbf{h}_r, \mathbf{t} \rangle$ between the relation-specific transformed head \mathbf{h}_r and tail \mathbf{t} . The model aims to minimize

the distance between \mathbf{h}_r and tail \mathbf{t} , *i.e.* their similarity $\langle \mathbf{h}_r, \mathbf{t} \rangle$ is maximized for positive triples. Otherwise, it is conversely minimized for sampled negative triples.

There are various ways to define the similarity $\langle \mathbf{h}_r, \mathbf{t} \rangle$. In this paper, we choose the following definitions for experiments.

Trace Distance.

The trace distance measures the distinguishability between two states. Two states are more similar if their trace distance is smaller. We define the similarity as the negative of the trace distance as

$$f(h, r, t) = -\frac{1}{2} \text{tr}(\sqrt{(\rho_{h_r} - \rho_t)^\dagger (\rho_{h_r} - \rho_t)}) \quad (9)$$

where ρ_{h_r}, ρ_t are the density matrices of states $|h_r\rangle$ and $|t\rangle$ respectively, $\text{tr}(\rho)$ is the trace of density matrix ρ , ρ^\dagger is the conjugate transpose of ρ .

Hilbert-Schmidt Distance.

Hilbert-Schmidt distance between two states is known as l_2 distance, while the l_1 distance is trace distance. Similarly, we define the similarity as the negative of the Hilbert-Schmidt distance as

$$f(h, r, t) = -\text{tr}((\rho_{h_r} - \rho_t)^\dagger (\rho_{h_r} - \rho_t)) \quad (10)$$

We also explore more definitions that may contribute to the training procedure. Element-wise l_1 distance and element-wise inner product are two measurements that follows previous classic KGEs.

Element-wise l_1 Distance.

$$f(h, r, t) = -\|\mathbf{h}_r - \mathbf{t}\|_1$$

$$= -\sum_{i=1}^d \|\mathbf{h}_{ri} - \mathbf{t}_i\|_1 \quad (11)$$

where $\|\mathbf{x}\|_1$ is the l_1 norm of the two-dimensional complex vector $\mathbf{x} \in \mathbb{C}^{2d}$.

Element-wise Inner Product.

$$f(h, r, t) = \text{Re}(\langle \mathbf{h}_r, \bar{\mathbf{t}} \rangle) \quad (12)$$

where $\text{Re}(\mathbf{x})$ is the real part of the two-dimensional complex vector $\mathbf{x} \in \mathbb{C}^{2d}$. $\langle \mathbf{h}_r, \bar{\mathbf{t}} \rangle$ is element-wise inner product.

4.1.4 Loss Function

In order to optimize the model, we formulate the link prediction task as a classification problem. Following (Sun et al., 2019), the model minimizes the

339 following loss:

$$\begin{aligned}
Loss &= -\log(\gamma - f(h, r, t)) \\
&- \sum_{i=1}^K p(h_i, r_i, t_i) \log \sigma(f(h_i, r_i, t_i) - \gamma)
\end{aligned}
\tag{13}$$

341 where γ is a fixed margin, K is the number
342 of negative examples, (h_i, r_i, t_i) is the i th neg-
343 ative triple, σ is the sigmoid function. Besides,
344 $p(h_i, r_i, t_i)$ is the distribution of sampling negative
345 samples and it depends on negative sampling strate-
346 gies such as uniform sampling, bernoulli sampling
347 and adversarial sampling (Sun et al., 2019).

348 4.1.5 Initialization

349 For parameter initialization, we adopt a particular
350 initialization algorithm to preserve quantum ada-
351 vantages and speed up model efficiency and conver-
352 gence (Glorot and Bengio, 2010). The initialization
353 of entities follows the rule:

$$\begin{aligned}
\mathbf{a}_{\text{real}} &= \cos(\theta) \\
\mathbf{a}_{\text{img}} &= \sin(\theta) \cos(\phi) \\
\mathbf{b}_{\text{real}} &= \sin(\theta) \sin(\phi) \cos(\varphi) \\
\mathbf{b}_{\text{img}} &= \sin(\theta) \sin(\phi) \sin(\varphi)
\end{aligned}
\tag{14}$$

355 where \mathbf{a}_{real} , \mathbf{a}_{img} , \mathbf{b}_{real} , \mathbf{b}_{img} denote the scalar and
356 imaginary coefficients of \mathbf{a} and \mathbf{b} , respectively.
357 θ, ϕ, φ are randomly generated from the interval
358 $[-\pi, \pi]$. The initialization of relations follows an
359 extended rule. The coefficients of \mathbf{a} and \mathbf{b} are ini-
360 tialized by the same rule as above, while the angle
361 ψ is randomly generated from the interval $[-\pi, \pi]$.
362 This initialization method is optional.

363 4.2 Theoretical Analysis

364 The Proposition 1 below illustrates the connection
365 with classic KGE methods.

366 **Proposition 1.** *qubit representation is equal to*
367 *unit quaternion representation. In this way, spe-*
368 *cial quantum gates are rotations in the quaternion*
369 *space.*

370 For each qubit representation, there are four free
371 variables normalized to 1. There exists a natural
372 one-to-one mapping ϕ :

$$\begin{aligned}
\phi : \mathbb{C}^{2d} &\rightarrow \mathbb{H}^d \\
(a + b\mathbf{i}) |0\rangle + (c + d\mathbf{i}) |1\rangle &\rightarrow a + b\mathbf{i} + c\mathbf{j} + d\mathbf{k} \\
a^2 + b^2 + c^2 + d^2 &= 1
\end{aligned}
\tag{15}$$

374 that map each qubit to unit quaternion. Similarly,
375 the relation representation is also mapped to unit
376 quaternion if we limit the angle $\psi = 0$ in unitary
377 matrix.

$$\begin{aligned}
\varphi : \mathbb{C}^{2 \times 2 \times d} &\rightarrow \mathbb{H}^d \\
\begin{pmatrix} a + b\mathbf{i} & -c + d\mathbf{i} \\ c + d\mathbf{i} & a - b\mathbf{i} \end{pmatrix} &\rightarrow a + b\mathbf{i} + c\mathbf{j} + d\mathbf{k} \\
a^2 + b^2 + c^2 + d^2 &= 1
\end{aligned}
\tag{16}$$

379 Therefore, that **special** quantum gates acting on
380 qubit states is equal to the Hamilton product of two
381 unit quaternions. With $\psi = 0$ we generate a variant
382 of QubitE, namely QubitE₂.

383 However, QuatE (Zhang et al., 2019) which rep-
384 represents entities as quaternion and relations as rota-
385 tions in the quaternion space, subsumes QubitE₂
386 but does not subsume QubitE, because the deter-
387 mine of unitary matrix representation of quantum
388 gates of QubitE is $e^{i\psi}$ rather than 1. In other words,
389 the general quantum gates of QubitE are not equal
390 to unit quaternions.

391 4.2.1 Subsumption

392 We show that QubitE subsumes other models and
393 inherits their favorable characteristics in learning
394 various graph patterns.

395 **Definition 1.** *A model M_1 subsumes M_2 when any*
396 *scoring over triples of a KG measured by model M_2*
397 *can also be obtained by M_1 (Wang et al., 2018).*

398 **Proposition 2.** *QubitE subsumes DistMult, pRo-*
399 *tatE, RotatE, TransE and ComplEx.*

400 4.2.2 Full Expressiveness

401 **Definition 2** (from (Kazemi and Poole, 2018)). *A*
402 *model M is fully expressive if there exist assign-*
403 *ments to the embeddings of the entities and*
404 *relations, that accurately separate correct triples for*
405 *any given ground truth.*

406 **Proposition 3.** *QubitE is fully expressive.*

407 4.2.3 Inference of Patterns

408 **Definition 3.** *Relation r_2 (e.g. StudentOf) is the*
409 *inversion of relation r_1 (e.g. SupervisorOf) if*

$$\forall x, y \in \mathcal{E}, (x, r_1, y) \in \mathcal{T} \Rightarrow (y, r_2, x) \in \mathcal{T}$$

411
412 **Proposition 4.** *Let $r_2 \in \mathcal{R}$ be the inversion of $r_1 \in$*
413 *\mathcal{R} . QubitE infers this pattern with $\mathcal{U}_{r_2, i} = \mathcal{U}_{r_1, i}^{-1}$*
414 *for $i = 1, 2, \dots, d$ where d is relation embedding*
415 *dimension.*

Definition 4. A relation r is symmetric (antisymmetric) if

$$\begin{aligned} \forall x, y \in \mathcal{E}, (x, r, y) \in \mathcal{T} &\Rightarrow (y, r, x) \in \mathcal{T} \\ ((x, r, y) \in \mathcal{T} &\Rightarrow (y, r, x) \notin \mathcal{T}) \end{aligned}$$

Proposition 5. Let $r \in \mathcal{R}$ be symmetric (antisymmetric). QubitE infers the symmetry (antisymmetry) pattern if $\mathfrak{U}_{r,i} = \mathfrak{U}_{r,i}^{-1}$ holds (does not hold) for $i = 1, 2, \dots, d$ where d is relation embedding dimension.

Definition 5. Relation r_1 and relation r_2 are commutative (non-commutative) if

$$\begin{aligned} \forall x, y \in \mathcal{E}, (x, r_1 \circ r_2, y) \in \mathcal{T} \\ \Rightarrow (x, r_2 \circ r_1, y) \in \mathcal{T} \\ (\exists x, y \in \mathcal{E}, (x, r_1 \circ r_2, y) \in \mathcal{T} \\ \Rightarrow (x, r_2 \circ r_1, y) \notin \mathcal{T}) \end{aligned}$$

where \circ is the composition operator.

Definition 6. Relation r_3 (e.g. UncleOf) is the composition of relation r_1 (e.g. FatherOf) and relation r_2 (e.g. BrotherOf) if

$$\begin{aligned} \forall x, y, z \in \mathcal{E}, (x, r_1, y) \in \mathcal{T} \wedge (y, r_2, z) \in \mathcal{T} \\ \Rightarrow (x, r_3, z) \in \mathcal{T} \end{aligned}$$

Proposition 6. Let $r_1, r_2, r_3 \in \mathcal{R}$ be relations and r_3 be a composition of r_1 and r_2 . QubitE infers composition with $\mathfrak{U}_{r_2,i}\mathfrak{U}_{r_1,i} = \mathfrak{U}_{r_3,i}$. If r_1 and r_2 are commutative, then $\mathfrak{U}_{r_2,i}\mathfrak{U}_{r_1,i} = \mathfrak{U}_{r_1,i}\mathfrak{U}_{r_2,i}$. If r_1 and r_2 are non-commutative, then $\mathfrak{U}_{r_2,i}\mathfrak{U}_{r_1,i} \neq \mathfrak{U}_{r_1,i}\mathfrak{U}_{r_2,i}$ for $i = 1, 2, \dots, d$ where d is relation embedding dimension.

With above propositions, we have the following theorem:

Theorem 1. QubitE can model the symmetry / antisymmetry, inversion, and commutative / non-commutative composition patterns.

4.2.4 Complexity Analysis

Table 1 compares the space and time complexity of QubitE with several popular models. It can be seen that QubitE is efficient and shares similar complexity with classical KGEs such as TransE, RotatE and QuatE, etc.

Methods	Space Complexity	Time Complexity
TransE	$O(\mathcal{E} n + \mathcal{R} n)$	$O(n)$
TransH	$O(\mathcal{E} n + \mathcal{R} n)$	$O(n)$
TransR	$O(\mathcal{E} n + \mathcal{R} n^2)$	$O(n^2)$
RESCAL	$O(\mathcal{E} n + \mathcal{R} n^2)$	$O(n^2)$
DistMult	$O(\mathcal{E} n + \mathcal{R} n)$	$O(n)$
ComplEx	$O(\mathcal{E} n + \mathcal{R} n)$	$O(n)$
RotatE	$O(\mathcal{E} n + \mathcal{R} n)$	$O(n)$
QuatE	$O(\mathcal{E} n + \mathcal{R} n)$	$O(n)$
5*E	$O(\mathcal{E} n + \mathcal{R} n)$	$O(n)$
QubitE	$O(\mathcal{E} n + \mathcal{R} n)$	$O(n)$

Table 1: Comparison in space and time complexity.

5 Experiments

5.1 Experimental Settings

Datasets We evaluated our model on four widely used benchmark datasets namely FB15k (Bollacker et al., 2008), FB15k-237 (Toutanova and Chen, 2015), WN18 (Bordes et al., 2013) and WN18RR (Dettmers et al., 2018). Table 2 summarises the statistics of these four datasets. FB15k is a standard benchmark created from the original FreeBase KG (Bollacker et al., 2008). WN18 (Bordes et al., 2013) is a lexical database with hierarchical collection for the English language that was derived from the original WordNet dataset (Miller, 1992). According to (Dettmers et al., 2018), FB15k and WN18 suffer from the test leakage problem. The training set contains a large number of inverse test triples. To solve the problem, FB15k-237 and WN18RR are proposed as sub-version of FB15k and WN18, respectively, with inverse relations removed. The FB15k-237 and WN18RR datasets both include several relational patterns such as composition (e.g. *awardnominee/.../nominatedfor*), symmetry (e.g. *derivationally_related_form* in WN18RR), and anti-symmetry (e.g. *has_part* in WN18RR).

Evaluation Protocol In order to speed up evaluation, we score each triple with all entities at a time. In detail, firstly, for each test triples, we replace tail entity with all entities in the KG to obtain candidate triples. Then, we compute the scores of all candidate triples and sort them by scores ascending order. Finally, we store the rank of the correct triple. Following the best practices of evaluations for em-

Dataset	#train	#valid	#test
FB15k	483,142	50,000	59,071
WN18	141,442	5,000	5,000
FB15k-237	272,115	17,535	20,466
WN18RR	86,835	3,034	3,134

Table 2: **Dataset Statistics.** Split of datasets in terms of number of triples.

bedding models, we consider the most-used metrics (Mean) Reciprocal Rank (MRR) and Hits@n (n = 1, 3, 10). For all metrics, the higher, the better.

Implementation Details We implement our model with PyTorch (Paszke et al., 2017). The model is trained and tested on one GTX1080 graphic card. We use Adam as a gradient optimizer. We do not use Dropout because it may lead normalization to 0 and destroy our normalization. See Appendix A.2 for more details.

Baselines We compare QubitE with a number of strong baselines. For *Euclidean KG Embedding*, we reported TransE (Bordes et al., 2013), TransR (Lin et al., 2015), RotatE (Sun et al., 2019), QuatE (Zhang et al., 2019), 5*E (Nayyeri et al., 2021) and HopfE (Bastos et al., 2021). For *Non-Euclidean KG Embedding*, we reported MuRP (Balazevic et al., 2019b) and ATTH (Chami et al., 2020). For *Tensor Decomposition KG Embedding*, we reported DistMult (Yang et al., 2015), ComplEx (Trouillon et al., 2016), Simple (Kazemi and Poole, 2018), Hyper (Balazevic et al., 2019a). For *Neural Network KG Embedding*, we reported ConvE (Dettmers et al., 2018), CoPER (Stoica et al., 2020). For *Quantum KG Embedding*, we reported QCE (Ma et al., 2019) and its variant F-QCE (Ma et al., 2019).

5.2 Experimental Results and Analysis

We study the performance of our method on link prediction task. Table 3 shows the results on WN18RR and FB15k-237, and Table 4 summarizes the results on WN18 and FB15k. Overall, QubitE achieves extremely competitive results compared to the state-of-the-art classical models on all metrics across all datasets.

FB15k-237 and WN18RR mainly contain inference patterns of symmetry/antisymmetry and composition. For Euclidean KGEs, TransE and TransR perform the worst because they cannot infer antisymmetry or inversion patterns. RotatE and its

variant pRotatE perform better for their inference ability. But QubitE subsumes RotatE and not surprisingly has better performance than RotatE. From RotatE, QuatE to HopfE, the MRR and Hits@10 steadily improve with the promotion on the complex space, quantization space, etc. For Tensor Decomposition KGEs, ComplEx and DistMult perform poorly since they cannot infer the composition pattern. For Neural Network KGEs, ConvE and CoPER utilise convolution neural network and contextual parameter generate neural network to score triples. But these two methods require too many parameters when compared to the linear model QubitE. On the whole, the improvement of our method demonstrate the high expressiveness of QubitE.

FB15k and WN18 mainly contain inference patterns of symmetry/antisymmetry and inversion. For Euclidean KGEs, TransE and TransR perform poorly on these two datasets because TransE cannot handle symmetry patterns and TransR cannot infer inversion patterns. RotatE converts the relation into the rotation in complex space, while QuatE in quaternion space. But as QuatE observes, the normalization of the relation to unit quaternion is a critical step for the embedding performance. And QubitE satisfies the normalization constraint naturally for quantum advantages, thus performing much better. All in all, QubitE preserves the quantum advantages and efficiently separates the qubit states.

As a quantum-based method, QubitE outperforms the two representative quantum-based models QCE and F-QCE significantly. Compared with QCE and F-QCE, QubitE gains 50% improvements in average across all metrics on FB15k and WN18. We believe the improvement of QubitE originate from its pattern inference ability, full-expressiveness, subsumption and the correct application of quantum mechanism on link prediction task.

6 Conclusion

In this paper, we propose a novel KG embedding model named *QubitE* to apply quantum mechanics for knowledge graph completion. QubitE models entities as qubit states and represents relations as quantum gates. With fine-grained initialization algorithm and scoring function, QubitE can preserve quantum advantages and separate the triples properly. With detailed theoretical analysis,

	WN18RR				FB15k-237			
	MRR	Hits@10	Hits@3	Hits@1	MRR	Hits@10	Hits@3	Hits@1
TransE (Bordes et al., 2013)	.226	.501	–	–	.294	.465	–	–
TransR (Lin et al., 2015)	–	.503	–	–	–	.486	–	–
RotatE (Sun et al., 2019)	.476	.571	.492	.428	.338	.533	.375	.241
QuatE (Zhang et al., 2019)	<u>.481</u>	.564	<u>.500</u>	<i>.436</i>	.311	.495	.342	.221
NagE (Yang et al., 2020)	.477	.574	<i>.493</i>	.432	.340	.530	<i>.378</i>	<i>.244</i>
5*E (Nayyeri et al., 2021)	.470	<u>.580</u>	<u>.500</u>	.410	<u>.350</u>	.530	.380	.260
HopfE (Bastos et al., 2021)	.472	.586	<u>.500</u>	.413	<i>.343</i>	<u>.534</u>	<u>.379</u>	<u>.247</u>
MuRP (Balazevic et al., 2019b)	.480	.570	<u>.500</u>	.440	.340	.520	.370	.240
ATTH (Chami et al., 2020)	.456	.526	.471	.419	.311	.488	.339	.223
DistMult◇ (Yang et al., 2015)	.430	.490	.440	.390	.241	.419	.263	.155
ComplEx◇ (Trouillon et al., 2016)	.440	.510	.460	.410	.247	.428	.275	.158
HypER (Balazevic et al., 2019a)	.465	.522	.477	<i>.436</i>	.341	.520	.376	.252
ConvE◇ (Dettmers et al., 2018)	.430	.520	.440	.400	.325	.501	.356	.237
CoPER (Stoica et al., 2020)	.465	.510	–	.427	.365	.504	–	.295
QCE (Ma et al., 2019)	–	.323	.195	–	–	.350	.225	–
F-QCE (Ma et al., 2019)	–	.378	.274	–	–	.337	.198	–
QubitE (ours)	.486	<i>.579</i>	.503	<u>.439</u>	.341	.536	<u>.379</u>	<i>.244</i>

Table 3: Link prediction results on WN18RR and FB15k-237. Results are grouped from top to bottom by Euclidean KGE, Non-Euclidean KGE, Tensor Decomposition KGE, Neural Network KGE and Quantum KGE. Best results are in bold, second best results are underlined, third best results are italic. [◇]: Results are taken from (Dettmers et al., 2018). Other results are taken from their original papers.

	WN18				FB15k			
	MRR	Hits@10	Hits@3	Hits@1	MRR	Hits@10	Hits@3	Hits@1
TransE (Bordes et al., 2013)	.495	.943	.888	.113	.463	.749	.578	.297
TransR (Lin et al., 2015)	.427	.940	.876	.335	.198	.582	.404	.218
RotatE (Sun et al., 2019)	<i>.949</i>	<u>.959</u>	.952	<i>.944</i>	.797	<i>.884</i>	.830	.746
QuatE (Zhang et al., 2019)	<i>.949</i>	.960	<u>.954</u>	.941	.770	.821	.778	.700
NagE (Yang et al., 2020)	<u>.950</u>	.960	.953	<i>.944</i>	–	–	–	–
5*E (Nayyeri et al., 2021)	<u>.950</u>	.960	.950	.950	.730	.860	.780	.660
HopfE (Bastos et al., 2021)	<i>.949</i>	.960	<u>.954</u>	.938	–	–	–	–
DistMult◇ (Yang et al., 2015)	.797	.893	–	–	.798	.893	–	–
ComplEx (Trouillon et al., 2016)	.941	.947	.936	.936	.692	.840	.759	.599
Simple (Kazemi and Poole, 2018)	.942	.947	.944	.939	.727	.838	.773	.660
HypER (Balazevic et al., 2019a)	.951	.958	.955	<u>.947</u>	<u>.790</u>	<u>.885</u>	<u>.829</u>	<u>.734</u>
ConvE (Dettmers et al., 2018)	.943	.956	.946	.935	.657	.831	.723	.558
QubitE (ours)	<i>.949</i>	.960	.953	<i>.944</i>	<i>.773</i>	<u>.885</u>	.826	<i>.703</i>

Table 4: Link prediction results on WN18 and FB15k. Results are grouped from top to bottom by Euclidean KGE, Tensor Decomposition KGE, Neural Network KGE. Best results are in bold, second best results are underlined, third best results are italic. [◇]: Results are taken from (Dettmers et al., 2018); Other results are taken from their original papers.

QubitE owns the advantages of full expressiveness, subsumption, pattern inference ability and linear space&time complexity. Empirical experimental evaluations on four well-established datasets show that QubitE achieves an overall comparable performance, outperforming multiple recent strong

baselines.

In the future, we would like to explore the following research directions: (1) we plan to model logical rules from the KG by using the learned embedding; (2) we plan to model complex logical query with more types of quantum gates.

References

- 594 Ivana Balazevic, Carl Allen, and Timothy M.
595 Hospedales. 2019a. [Hypernetwork knowledge
596 graph embeddings](#). In *Artificial Neural Networks
597 and Machine Learning - ICANN 2019 - 28th Inter-
598 national Conference on Artificial Neural Networks,
599 Munich, Germany, September 17-19, 2019, Proceed-
600 ings - Workshop and Special Sessions*, volume 11731
601 of *Lecture Notes in Computer Science*, pages 553–
602 565. Springer.
- 603 Ivana Balazevic, Carl Allen, and Timothy M.
604 Hospedales. 2019b. [Multi-relational poincaré graph
605 embeddings](#). In *Advances in Neural Informa-
606 tion Processing Systems 32: Annual Conference
607 on Neural Information Processing Systems 2019,
608 NeurIPS 2019, December 8-14, 2019, Vancouver,
609 BC, Canada*, pages 4465–4475.
- 610 Ivana Balazevic, Carl Allen, and Timothy M.
611 Hospedales. 2019c. [Tucker: Tensor factorization
612 for knowledge graph completion](#). In *Proceedings
613 of the 2019 Conference on Empirical Methods in
614 Natural Language Processing and the 9th Interna-
615 tional Joint Conference on Natural Language Pro-
616 cessing, EMNLP-IJCNLP 2019, Hong Kong, China,
617 November 3-7, 2019*, pages 5184–5193. Association
618 for Computational Linguistics.
- 619 Anson Bastos, Kuldeep Singh, Abhishek Nadgeri,
620 Saeedeh Shekarpour, Isaiah Onando Mulang, and
621 Johannes Hoffart. 2021. [Hopfe: Knowledge graph
622 representation learning using inverse hopf fibrations](#).
623 In *Proceedings of the 30th ACM International Con-
624 ference on Information & Knowledge Management,
625 CIKM '21*, page 89–99, New York, NY, USA. Asso-
626 ciation for Computing Machinery.
- 627 Kurt Bollacker, Colin Evans, Praveen Paritosh, Tim
628 Sturge, and Jamie Taylor. 2008. [Freebase: A collab-
629 oratively created graph database for structuring hu-
630 man knowledge](#). In *Proceedings of the 2008 ACM
631 SIGMOD International Conference on Management
632 of Data, SIGMOD '08*, page 1247–1250, New York,
633 NY, USA. Association for Computing Machinery.
- 634 Antoine Bordes, Nicolas Usunier, Alberto García-
635 Durán, Jason Weston, and Oksana Yakhnenko.
636 2013. Translating embeddings for modeling multi-
637 relational data. In *NIPS 2013*.
- 638 Ines Chami, Adva Wolf, Da-Cheng Juan, Frederic
639 Sala, Sujith Ravi, and Christopher Ré. 2020. [Low-
640 dimensional hyperbolic knowledge graph embed-
641 dings](#). In *Proceedings of the 58th Annual Meeting of
642 the Association for Computational Linguistics, ACL
643 2020, Online, July 5-10, 2020*, pages 6901–6914.
644 Association for Computational Linguistics.
- 645 Tim Dettmers, Pasquale Minervini, Pontus Stenetorp,
646 and Sebastian Riedel. 2018. [Convolutional 2d
647 knowledge graph embeddings](#). In *Proceedings of
648 the Thirty-Second AAAI Conference on Artificial
649 Intelligence, (AAAI-18), the 30th innovative Ap-
650 plications of Artificial Intelligence (IAAI-18), and
651 the 8th AAAI Symposium on Educational Advances
652 in Artificial Intelligence (EAAI-18), New Orleans,
653 Louisiana, USA, February 2-7, 2018*, pages 1811–
654 1818. AAAI Press.
- Xavier Glorot and Yoshua Bengio. 2010. Understand-
655 ing the difficulty of training deep feedforward neural
656 networks. In *Proceedings of the thirteenth interna-
657 tional conference on artificial intelligence and statis-
658 tics*, pages 249–256. JMLR Workshop and Confer-
659 ence Proceedings. 660
- Jamie Heredge, Charles Hill, Lloyd Hollenberg, and
661 Martin Sevier. 2021. Quantum support vector ma-
662 chines for continuum suppression in b meson decays.
663 *arXiv e-prints*, pages arXiv–2103. 664
- Seyed Mehran Kazemi and David Poole. 2018. [Simple
665 embedding for link prediction in knowledge graphs](#).
666 In *Advances in Neural Information Processing Sys-
667 tems 31: Annual Conference on Neural Information
668 Processing Systems 2018, NeurIPS 2018, December
669 3-8, 2018, Montréal, Canada*, pages 4289–4300. 670
- Yankai Lin, Zhiyuan Liu, Maosong Sun, Yang Liu, and
671 Xuan Zhu. 2015. Learning entity and relation em-
672 beddings for knowledge graph completion. In *AAAI
673 2015*. 674
- Seth Lloyd, Maria Schuld, Aroosa Ijaz, Josh Izaac,
675 and Nathan Killoran. 2020. Quantum embed-
676 dings for machine learning. *arXiv preprint
677 arXiv:2001.03622*. 678
- Yunpu Ma, Volker Tresp, Liming Zhao, and Yuyi Wang.
679 2019. [Variational quantum circuit model for knowl-
680 edge graph embedding](#). *Advanced Quantum Tech-
681 nologies*, 2(7-8):1800078. 682
- George A. Miller. 1992. Wordnet: A lexical database
683 for english. *Commun. ACM*, 38:39–41. 684
- Mojtaba Nayyeri, Sahar Vahdati, Can Aykul, and
685 Jens Lehmann. 2021. [5* knowledge graph embed-
686 dings with projective transformations](#). *Proceedings
687 of the AAAI Conference on Artificial Intelligence*,
688 35(10):9064–9072. 689
- Adam Paszke, Sam Gross, Soumith Chintala, Gregory
690 Chanan, Edward Yang, Zachary DeVito, Zeming
691 Lin, Alban Desmaison, Luca Antiga, and Adam
692 Lerer. 2017. Automatic Differentiation in PyTorch.
693 In *NIPS-W*. 694
- Bernhard Schölkopf, Alexander J Smola, Francis Bach,
695 et al. 2002. *Learning with kernels: support vector
696 machines, regularization, optimization, and beyond*.
697 MIT press. 698
- Maria Schuld. 2021. Quantum machine learning mod-
699 els are kernel methods. *arXiv e-prints*, pages arXiv–
700 2101. 701
- George Stoica, Otilia Stretcu, Emmanouil Antonios
702 Platanios, Tom Mitchell, and Barnabás Póczos. 703

2020. Contextual parameter generation for knowledge graph link prediction. In *Proceedings of the AAAI Conference on Artificial Intelligence*, volume 34, pages 3000–3008.

Zhiqing Sun, Zhi-Hong Deng, Jian-Yun Nie, and Jian Tang. 2019. [Rotate: Knowledge graph embedding by relational rotation in complex space](#). In *International Conference on Learning Representations*.

Kristina Toutanova and Danqi Chen. 2015. Observed versus latent features for knowledge base and text inference.

Théo Trouillon, Johannes Welbl, Sebastian Riedel, Éric Gaussier, and Guillaume Bouchard. 2016. [Complex embeddings for simple link prediction](#). In *Proceedings of the 33rd International Conference on Machine Learning, ICML 2016, New York City, NY, USA, June 19-24, 2016*, volume 48 of *JMLR Workshop and Conference Proceedings*, pages 2071–2080. JMLR.org.

Yanjie Wang, Rainer Gemulla, and Hui Li. 2018. On multi-relational link prediction with bilinear models. In *AAAI*.

Bishan Yang, Wen-tau Yih, Xiaodong He, Jianfeng Gao, and Li Deng. 2015. [Embedding entities and relations for learning and inference in knowledge bases](#). In *3rd International Conference on Learning Representations, ICLR 2015, San Diego, CA, USA, May 7-9, 2015, Conference Track Proceedings*.

Tong Yang, Long Sha, and Pengyu Hong. 2020. [Nage: Non-abelian group embedding for knowledge graphs](#). In *Proceedings of the 29th ACM International Conference on Information & Knowledge Management, CIKM '20*, page 1735–1742, New York, NY, USA. Association for Computing Machinery.

Shuai Zhang, Yi Tay, Lina Yao, and Qi Liu. 2019. [Quaternion knowledge graph embeddings](#). In *Advances in Neural Information Processing Systems*, volume 32. Curran Associates, Inc.

A Appendix

A.1 Theoretical Proofs

A.1.1 Subsumption

Here we will prove Proposition 2. We will show that QubitE subsumes DistMult, pRotatE, RotatE, TransE and ComplEx and inherits their favorable characteristics in learning various graph patterns.

Before our proof for Proposition 2, we give the proposition below:

Proposition 7. \forall unit quaternion q , there exists a surjection $\phi : \mathbb{H} \rightarrow \mathbb{C}$ such that $\phi(q)$ is complex number. Moreover, $\phi(q)$ can be written in quaternion format $\phi(q) = a + 0\mathbf{i} + b\mathbf{j} + 0\mathbf{k}$, $a, b \in \mathbb{R}$, and

the Hamilton product in quaternion space will also degrade to complex number multiplication.

Proof. For any given unit quaternion $q = a + b\mathbf{i} + c\mathbf{j} + d\mathbf{k}$, we can write:

$$\begin{aligned} a &= \cos(\theta) \\ b &= \sin(\theta) \cos(\phi) \\ c &= \sin(\theta) \sin(\phi) \cos(\varphi) \\ d &= \sin(\theta) \sin(\phi) \sin(\varphi) \end{aligned} \tag{17}$$

where $\theta, \phi, \varphi \in [-\pi, \pi]$. Our goal is to generate $\phi(q) = a' + 0\mathbf{i} + b'\mathbf{j} + 0\mathbf{k}$ where $a', b' \in \mathbb{R}$.

First, we can generate a' from a with

$$a' = \frac{a}{1 - a^2}. \tag{18}$$

which implies $a' \in \mathbb{R}$.

Second, we note that

$$\begin{aligned} \frac{c}{b} &= \tan(\phi) \cos(\varphi), \\ \frac{d}{b} &= \tan(\phi) \sin(\varphi) \\ \frac{c^2}{b^2} + \frac{d^2}{b^2} &= \tan^2(\phi) \\ \frac{c^2}{b} + \frac{d^2}{b} &= b \left(\frac{c^2}{b^2} + \frac{d^2}{b^2} \right) \\ &= \sin(\theta) \cos(\phi) \tan^2(\phi) \in \mathbb{R} \end{aligned} \tag{19}$$

Therefore, we can generate b' with b, c, d with

$$b' = \frac{c^2}{b} + \frac{d^2}{b} \tag{20}$$

which implies $b' \in \mathbb{R}$. The surjection is

$$\begin{aligned} \phi : \mathbb{H} &\rightarrow \mathbb{C} \\ a + b\mathbf{i} + c\mathbf{j} + d\mathbf{k} &\rightarrow a' + 0\mathbf{i} + b'\mathbf{j} + 0\mathbf{k} \\ a' &= \frac{a}{1 - a^2} \\ b' &= \frac{c^2}{b} + \frac{d^2}{b} \end{aligned} \tag{21}$$

and the Hamilton product in quaternion space will also degrade to complex number multiplication. \square

Then we can begin our proof for Proposition 2.

Proof. For any given entity h and relation r , we have proved that they can be mapped to unit quaternions naturally (See Proposition 1). For any unit

quaternions, we also prove that there exists a surjection that maps to complex numbers (See Proposition 7). Let $\mathbf{z}_e = a'_e + 0\mathbf{i} + b'_e\mathbf{j} + 0\mathbf{k}$ where e represents qubit states, \mathbf{z}_e is the projected quaternion format of e . Therefore, we obtain the following equation:

$$\begin{aligned}
f(h, r, t) &= \text{Re}(\langle \mathbf{h}_r, \bar{\mathbf{t}} \rangle) \\
&= \text{Re}(\langle \mathbf{z}_{h_r}, \bar{\mathbf{z}}_{\mathbf{t}} \rangle) \\
&= \sum_{i=1}^d \text{Re}(\langle \mathbf{z}_{h_{r_i}}, \bar{\mathbf{z}}_{\mathbf{t}_i} \rangle) \\
&= \sum_{i=1}^d \text{Re}(\langle \mathbf{z}_{h_i}, \mathbf{z}_{r_i}, \bar{\mathbf{z}}_{\mathbf{t}_i} \rangle) \\
&= f_{\text{Complex}}(h, r, t)
\end{aligned} \tag{22}$$

which shows that QubitE subsumes Complex. By removing the imaginary parts of \mathbf{z}_e , the scoring function becomes $f(h, r, t) = \sum_{i=1}^d \langle \text{Re}(\mathbf{z}_{h_i}), \text{Re}(\mathbf{z}_{r_i}), \text{Re}(\mathbf{z}_{\mathbf{t}_i}) \rangle$, degrading to DistMult in this case. On the other hand, we also have the following equation:

$$\begin{aligned}
f(h, r, t) &= -\|\mathbf{h}_r - \mathbf{t}\| \\
&= -\|\mathbf{z}_{h_r} - \mathbf{z}_{\mathbf{t}}\| \\
&= -\|\mathbf{z}_h \circ \mathbf{z}_r - \mathbf{z}_{\mathbf{t}}\| \\
&= f_{\text{RotatE}}(h, r, t)
\end{aligned} \tag{23}$$

which shows that QubitE subsumes RotatE. From (Sun et al., 2019) we know RotatE subsumes pRotatE and TransE. So QubitE also subsumes pRotatE and TransE. \square

A.1.2 Full Expressiveness

Here we prove Proposition 3, that QubitE is fully expressive.

Proof. The proof contains two steps. First, we show that QubitE is expressive. Second, we show that the expressiveness is full.

In formulation, first, we show that QubitE can express any ranking tensor $\mathcal{A} \in \mathbb{R}^{n_e \times n_e \times n_r}$ where n_e is the number of entities and n_r is number of relations in KG. The ikj -th element of \mathcal{A} , denoted α_{ikj} , corresponds to the triple (h_i, r_k, t_j) . The ranking tensor gives lower rank to the triple (h_i, r_k, t_j) than to (h'_i, r'_k, t'_j) if the model scores the triple (h_i, r_k, t_j) higher than (h'_i, r'_k, t'_j) . Second, for any boolean tensor $\mathcal{B} \in \{0, 1\}^{n_e \times n_e \times n_r}$, QubitE obtains a ranking tensor which is consistent with \mathcal{B} . That is, for $\beta_{ikj} = 1$ where the triple (h_i, r_k, t_j) is positive and $\beta_{i'k'j'} = 0$ where the triple (h'_i, r'_k, t'_j)

is negative, we have $\alpha_{ikj} > \alpha_{i'k'j'}$ to correctly separate the triples.

For the first step, Wang et al. (2018) proved that the Complex model can obtain score tensor $\mathcal{M}^{n_e \times n_e \times n_r}$ that fullfills the ranking rules. The model gives score $\mu_{ikj} = f(h_i, r_k, t_j)$ for triple (h_i, r_k, t_j) , such that $\mu_{ikj} < \mu_{i'k'j'}$ holds for the definition of ranking tensor \mathcal{A} . In the subsumption 2 we proved that QubitE subsumes Complex. Therefore, there is a vector assignment to embeddings of entities and relations such that QubitE obtains a ranking tensor.

For the second step, Wang et al. (2018) show that for a given boolean matrix \mathcal{B} , there exists a ranking matrix consistent with \mathcal{B} . Therefore, it is also true for QubitE to obtain a ranking matrix consistent with \mathcal{B} .

With the first and the second step, we conclude that there exists an assignment to entity and relation embeddings such that for any ground truth, QubitE can separate the triples correctly. This means QubitE is fully expressive. \square

A.1.3 Inference of Patterns

Symmetry/Antisymmetry

Definition 7. A relation r is symmetric (antisymmetric) if

$$\begin{aligned}
\forall x, y \in \mathcal{E}, (x, r, y) \in \mathcal{T} &\Rightarrow (y, r, x) \in \mathcal{T} \\
((x, r, y) \in \mathcal{T} &\Rightarrow (y, r, x) \notin \mathcal{T})
\end{aligned}$$

Proposition 8. Let $r \in \mathcal{R}$ be symmetric (antisymmetric). QubitE infers the symmetry (antisymmetry) pattern if $\mathfrak{U}_{r,i} = \mathfrak{U}_{r,i}^{-1}$ holds (does not hold) for $i = 1, 2, \dots, d$ where d is relation embedding dimension.

Proof. Firstly, we consider the situation that relation r is symmetric.

According to Definition 7, a model infers the symmetry pattern when for all given entities x, y , if (x, r, y) is represented as positive, then (y, r, x) is also represented as positive. That is

$$g_{r,i}(\mathbf{x}_i) = \mathbf{y}_i \tag{24}$$

then $g_{r,i}(\mathbf{y}_i) = \mathbf{x}_i$. From Equation 24, we have $\mathbf{y}_i = g_{r,i}(\mathbf{x}_i) = \mathfrak{U}_{r,i}\mathbf{x}_i$. Since $g_{r,i}$ is the quantum gate whose matrix representation $\mathfrak{U}_{r,i}$ is unitary and invertible, we can make the assumption $\mathfrak{U}_{r,i} = \mathfrak{U}_{r,i}^{-1}$ following Proposition 8. Then we have

$$\mathbf{y}_i = g_{r,i}^{-1}(\mathbf{x}_i) \tag{25}$$

which equals to $\mathbf{x}_i = g_{r,i}(\mathbf{y}_i)$. This means that the triple (y, r, x) must be positive, *i.e.* inferred as positive.

Secondly, if relation r is antisymmetric, we just make the assumption $\mathfrak{U}_{r,i} \neq \mathfrak{U}_{r,i}^{-1}$ to get $\mathbf{x}_i \neq g_{r,i}(\mathbf{y}_i)$, which means that the triple (y, r, x) is inferred as negative. \square

Inversion

Definition 8. Relation r_2 (e.g. *StudentOf*) is the inversion of relation r_1 (e.g. *SupervisorOf*) if

$$\forall x, y \in \mathcal{E}, (x, r_1, y) \in \mathcal{T} \Rightarrow (y, r_2, x) \in \mathcal{T}$$

Proposition 9. Let $r_2 \in \mathcal{R}$ be the inversion of $r_1 \in \mathcal{R}$. QubitE infers this pattern with $\mathfrak{U}_{r_2,i} = \mathfrak{U}_{r_1,i}^{-1}$ for $i = 1, 2, \dots, d$ where d is relation embedding dimension.

Proof. According to Definition 8, a model infers the inversion pattern when for all given entities x, y , if (x, r_1, y) is represented as positive, then (y, r_2, x) is also represented as positive. That is

$$g_{r_1,i}(\mathbf{x}_i) = \mathbf{y}_i \quad (26)$$

then $g_{r_2,i}(\mathbf{y}_i) = \mathbf{x}_i$. From Equation 26, we have $\mathbf{y}_i = g_{r_1,i}(\mathbf{x}_i) = \mathfrak{U}_{r_1,i}\mathbf{x}_i$. Since r_1 is the quantum gate whose matrix representation $\mathfrak{U}_{r_1,i}$ is unitary and invertible, we can make the assumption $\mathfrak{U}_{r_2,i} = \mathfrak{U}_{r_1,i}^{-1}$ following Proposition 9. Then we have

$$\mathbf{y}_i = g_{r_2,i}^{-1}(\mathbf{x}_i) \quad (27)$$

which equals to $\mathbf{x}_i = g_{r_2,i}(\mathbf{y}_i)$. This means that the triple (y, r_2, x) must be positive, *i.e.* inferred as positive. \square

Commutative/Non-commutative Composition

Definition 9. Relation r_1 and relation r_2 are commutative (non-commutative) if

$$\begin{aligned} \forall x, y \in \mathcal{E}, (x, r_1 \circ r_2, y) \in \mathcal{T} \\ \Rightarrow (x, r_2 \circ r_1, y) \in \mathcal{T} \\ (\exists x, y \in \mathcal{E}, (x, r_1 \circ r_2, y) \in \mathcal{T} \\ \Rightarrow (x, r_2 \circ r_1, y) \notin \mathcal{T}) \end{aligned}$$

where \circ is the composition operator.

Definition 10. Relation r_3 (e.g. *UncleOf*) is the composition of relation r_1 (e.g. *FatherOf*) and relation r_2 (e.g. *BrotherOf*) if

$$\begin{aligned} \forall x, y, z \in \mathcal{E}, (x, r_1, y) \in \mathcal{T} \wedge (y, r_2, z) \in \mathcal{T} \\ \Rightarrow (x, r_3, z) \in \mathcal{T} \end{aligned}$$

Proposition 10. Let $r_1, r_2, r_3 \in \mathcal{R}$ be relations and r_3 be a composition of r_1 and r_2 . QubitE infers composition with $\mathfrak{U}_{r_2,i}\mathfrak{U}_{r_1,i} = \mathfrak{U}_{r_3,i}$. If r_1 and r_2 are commutative, then $\mathfrak{U}_{r_2,i}\mathfrak{U}_{r_1,i} = \mathfrak{U}_{r_1,i}\mathfrak{U}_{r_2,i}$. If r_1 and r_2 are non-commutative, then $\mathfrak{U}_{r_2,i}\mathfrak{U}_{r_1,i} \neq \mathfrak{U}_{r_1,i}\mathfrak{U}_{r_2,i}$ for $i = 1, 2, \dots, d$ where d is relation embedding dimension.

Proof. According to Definition 6, a model infers a composition pattern when for all given entities x, y, z , if the score of the model represents triples (x, r_1, y) and (y, r_2, z) as positive, it also represents (x, r_3, z) as positive. In other words, when given

$$\begin{aligned} g_{r_1,i}(\mathbf{x}_i) &= \mathbf{y}_i \\ g_{r_2,i}(\mathbf{y}_i) &= \mathbf{z}_i \end{aligned} \quad (28)$$

then it holds $g_{r_3,i}(\mathbf{x}_i) = \mathbf{z}_i$ for $i = 1, 2, \dots, d$ where

$$\begin{aligned} g_{r_3,i}(\mathbf{h}_i) &= \mathfrak{U}_{r_2,i}\mathfrak{U}_{r_1,i}\mathbf{h}_i, \\ j &= 1, 2, 3; i = 1, 2, \dots, d \end{aligned} \quad (29)$$

From Equation 28, we insert $\mathbf{y}_i = g_{r_1,i}(\mathbf{x}_i)$ into $g_{r_2,i}(\mathbf{y}_i) = \mathbf{z}_i$, which gives $g_{r_2,i}(g_{r_1,i}(\mathbf{x}_i)) = \mathbf{z}_i$. Therefore, we have

$$g_{r_2,i} \circ g_{r_1,i}(\mathbf{x}_i) = \mathfrak{U}_{r_2,i}\mathfrak{U}_{r_1,i}\mathbf{x}_i = \mathbf{z}_i. \quad (30)$$

Considering the Proposition 6 and assuming $\mathfrak{U}_{r_2,i}\mathfrak{U}_{r_1,i} = \mathfrak{U}_{r_3,i}$, we have $g_{r_2,i} \circ g_{r_1,i}(\mathbf{x}_i) = g_{r_3,i}(\mathbf{x}_i) = \mathbf{z}_i$. This means that the triple (x, r_3, z) must be positive, *i.e.* inferred to be positive. If r_1 and r_2 are commutative, then $\mathfrak{U}_{r_2,i}\mathfrak{U}_{r_1,i} = \mathfrak{U}_{r_1,i}\mathfrak{U}_{r_2,i}$. If r_1 and r_2 are non-commutative, then $\mathfrak{U}_{r_2,i}\mathfrak{U}_{r_1,i} \neq \mathfrak{U}_{r_1,i}\mathfrak{U}_{r_2,i}$. \square

A.2 Implementation Details

We implement our model with PyTorch (Paszke et al., 2017). The model is trained and tested on one GTX1080 graphic card. We use Adam as a gradient optimizer. We do not use Dropout because it may lead normalization to 0 and destroy our normalization. We use grid search to obtain the best hyperparameters according to MRR on the validation set. The hyperparameters are selected as follows: embedding dimension $n \in \{100, 200, 500, 1000\}$, fixed margin $\gamma \in \{3, 6, 9, 12, 24\}$, self-adversarial sampling temperature $\alpha \in \{0.5, 1.0\}$, batch size $B \in \{256, 512, 1024\}$.

Table 5 shows the hyper-parameter values reported for QubitE across all datasets, where lr denotes (learning rate), dr (decay rate), ls (label smoothing), p (γ in loss function), neg (negative sample size), strategy (negative sampling strategy).

Dataset	lr	dr	d_e	d_r	p	neg	strategy
FB15k	0.00005	0.99	500	500	24	256	adversarial
FB15k-237	0.0005	0.995	500	500	12	256	adversarial
WN18	0.0001	0.995	500	500	12	256	uniform
WN18RR	0.00005	1.0	500	500	6	256	uniform

Table 5: Hyper-parameter values for QubitE across all datasets.

951 A.3 Limitation

952 On the one hand, one entity is only represented by
953 one qubit. There exists multi qubits system, that
954 represents entities as multi qubits and brings more
955 favorable features, though the theoretical analysis
956 becomes difficult. On the other hand, the conver-
957 gence is really slow because of thie slow sampling
958 procedure.